

Assessment of Bridge Performance - Seismic Isolation versus Ductility

A. Fäcke¹, M. Baur², and F.H. Schlüter¹

¹ *SMP Ingenieure im Bauwesen GmbH, Karlsruhe, Germany*

² *Dept. of Structural Engineering, University of Applied Sciences and Arts, Lucerne, Switzerland*
Email: a.faecke@smp-ing.de, michael.baur@hslu.ch

ABSTRACT :

Severe earthquake events are still marked by the collapse of bridges due to an inductile structural performance. In order to reach a high level of seismic safety and an economical design these structures should be able to dissipate a significant amount of the input energy, so that seismic forces are reduced. Energy dissipation can either be achieved by a ductile structural performance via plastic hinges in the piers or by seismic isolation using specific high damping rubber bearings. To both problems, which are linked together in practice, enhanced material laws were formulated describing the non-linear material behavior of reinforced concrete and elastomer subjected to cyclic loading.

The nonlinear behavior of reinforced concrete piers is modeled using the fibre beam theory. That theory was extended by a bond-slip approach, so that e.g. anchorages of reinforcement can more realistically be considered. In order to facilitate an objective simulation of large deformations with material softening a nonlocal damage approach from continuum mechanics was implemented.

For the modeling of the high damping rubber bearings an enhanced finite visco-elastic material law with an isotropic damage function was developed. Due to the fact, that elastomer is almost incompressible, the constitutive law is based on the uncoupling of the stress response into a linear volumetric and into a non-linear deviatoric part. The latter is described mathematically by a relaxation function and a distortion-supported damage function.

In this work the upgrading procedures and the effectiveness of both approaches will be discussed on the basis of realistic earthquake scenarios.

KEYWORDS:

Concrete, pier, nonlocal, elastomer, bridge bearing, finite elements

1. INTRODUCTION

The last strong earthquakes have again shown that bridges are still highly vulnerable due to an inductile structural performance. In particular bridges which are part of important infrastructure are necessary for rescue work and recovering measures and should therefore have a high level of seismic safety. In order to reach this aim these structures should be able to dissipate a significant amount of the input energy in order to reduce seismic forces and allow an economical design. Energy dissipation can either be achieved by a ductile structural performance thru the formation of plastic hinges in the piers or by seismic isolation using specific high damping rubber bearings. To both problems, which are linked together in practice, enhanced material laws could be formulated describing the nonlinear material behavior of reinforced concrete (RC) and elastomer subjected to cyclic loading. The nonlinear behavior in plastic hinges of reinforced concrete piers is modeled using the fibre beam theory. The conventional fibre theory was extended by a bond-slip approach, so that slip e.g. at anchorages of reinforcement can more realistically be considered. In order to facilitate an objective simulation of large pier deformations with material softening a nonlocal damage approach from continuum mechanics was implemented in the fibre beam element. With that approach the model shows good agreement to experimental results up to complete failure of the piers. For the modeling of the high damping rubber bearings an enhanced finite visco-elastic material law with an isotropic damage function was developed. Due to the fact, that elastomer is almost incompressible, the constitutive law is based on the uncoupling of the stress response into a linear volumetric and into a non-linear deviatoric part. The latter is described mathematically by a relaxation function and a distortion-supported damage function. In this work the effectiveness for the assessment and the upgrading procedure using both approaches will be discussed on the basis of realistic scenarios.

2. MODELING OF RC PIERS

The primary cause of nonlinearity in RC structures is cracking in tension and crushing in compression of concrete and yielding of reinforcement. The bond resistance between concrete and steel contributes to nonlinearity especially in the region of cracks and at anchorages of reinforcement. These characteristics were considered in a combined plasticity and damage model, which is briefly summarized below. A detailed description of the model can be taken from [Fäcke] and [Fäcke et al.].

2.1 Concrete

The stress strain relation for first loading in compression is described acc. to [Salse et al.]:

$$\sigma = \frac{E_0 \cdot \varepsilon}{1 + \left(\frac{f_{cm} \cdot E_0}{\varepsilon_1} - \frac{n}{n-1} \right) \cdot \left(\frac{\varepsilon}{\varepsilon_1} \right) + \frac{1}{n-1} \cdot \left(\frac{\varepsilon}{\varepsilon_1} \right)^n} \quad (2.1)$$

where E_0 is the tangent modulus at the origin of the stress-strain curve, f_{cm} is the mean cylinder compressive strength, ε_1 is the strain at compressive strength, and n is a factor for calibration to test data. This function also represents the envelope for all further un- and reloading cycles. The un- and reloading in compression is approximated linear elastic and decreases with increasing compression strain. The reduced tangent modulus E_{red} for un- and reloading takes the increasing damage due to concrete crushing into account.

Loading in tension is first linear elastic and then an exponential law is used for strain softening. Strain softening is based on the fictitious crack model proposed by Hillerborg using the fracture energy G_f . The tensile strength is linearly reduced from f_{ctm} to zero with increasing plastic compression strain ε_{pl} acc to Figure 1. The origin of the characteristic stress-strain curve in tension always moves to the actual plastic strain ε_{pl} . Contact effects in cracks are considered with an increase of compression stress before complete closure of cracks respectively before ε_{pl} is reached.

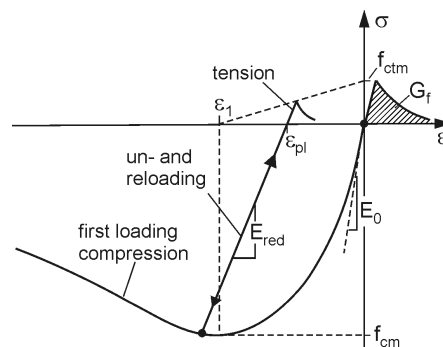


Figure 1 Cyclic stress strain relation of concrete

2.2 Steel

A nonlinear stress-strain curve for first loading is implemented in the constitutive equations of reinforcement that is basically based on the Ramberg Osgood curve for cold-formed steel. Because there is no distinct transition from elastic to plastic response at first loading, the yield point f_y is defined at 0.2% plastic strain. The stress strain characteristic for cyclic loading is based on the model of Ma et al. In this model an early yielding upon load reversal is considered constituting the Bauschinger effect. Further load reversals again consider the early yielding by following the stress strain curve of the previous load cycle rotated by 180°.

2.3 Bond Resistance

The idealized inelastic and nonlinear bond-slip relation for generalized excitation was implemented acc. to Eligehausen et al. It reproduces the successive deterioration of bond due to slip parallel to the bar axis. It starts from adhesion between steel and concrete over initiation of cone-shaped cracks around the reinforcing bar up to

crushing of concrete in front of the bar rips. A sufficient confinement through stirrups is anticipated so that no brittle splitting failure has to be expected. A complete crushing of the surrounding concrete results in a small frictional resistance. Deterioration through cyclic loading is dependent on maximum slip and dissipated energy.

2.4 Finite Element Model

Except for the confining pressure at stirrups, and potential torsional effects the stress field in slender piers is mainly unidirectional and parallel to its centerline. Hence the fibre beam element is a computationally effective formulation for the representation of the seismic pier performance. The cross section of that beam element is divided into a grid of integration points (fibres). Because different stress-strain curves can be assigned to the integration points, it is possible to consider the confining effect of the stirrups. Integration points inside the confined core of the section have a stress strain relation with higher strength and ductility than the integration points of the concrete cover.

Generally the reinforcement is considered by assigning a steel stress-strain curve to the corresponding integration points. However in this way it is not possible to assess the damage of bond through slip between steel and concrete. Hence in this work the reinforcement was considered by extra truss elements. The truss elements are connected to four node bond elements that are once more linked by rigid connections to the fibre elements. The pier is divided into sections that always contain the same set of elements (Figure 3).

The model is implemented in the FE-code ABAQUS. However, it can be implemented in any FE-code that offers the following features. For the fibre elements the number of section integration points of conventional beam elements must be selectable. For the 4-node bond element user defined elements can be implemented via subroutines.

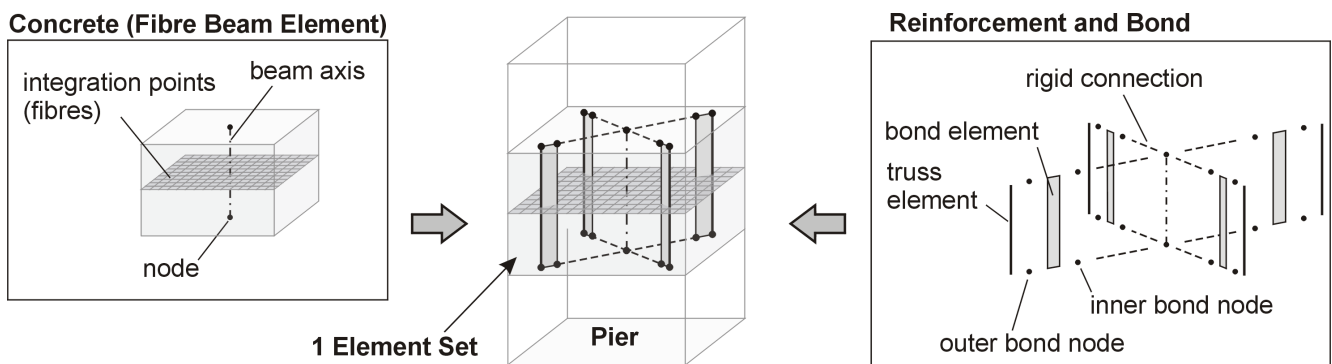


Figure 3 Finite element model of RC pier considering slip of main reinforcement.

2.5 Failure and Material Softening

The investigation of earthquake loading at RC structures involves large deformations close to structural failure. The macroscopic behavior of concrete then exhibits strain softening (i.e. a decrease of stress at increasing strain) in compression due to crushing and in tension due to crack initiation. In the classical finite element theory the negative tangential stiffness modulus causes a localization of damage or strain into a band of single elements or in the present case of one-dimensional problems in one element set. This leads to spurious mesh sensitivity, where the failure of the model occurs earlier and faster with increasing mesh refinement.

In order to avoid mesh sensitivity the nonlocal concept acc. to [Bazant et al.] was adapted to the fibre beam element for strain softening in compression. In this concept the stress in one integration point not only depends on the strain in this point but also from the strain in the neighboring points. In the present model the strain in the integration points of one element n is averaged with the corresponding strains of the elements above and below using a bell-shaped weight function. Therefore the influence of the surrounding elements on element n decreases with increasing distance and vanishes at distance R . The characteristic length R mainly depends on the material and on structural dimensions and was chosen in the simulations with 0.25 m.

3. CONSTITUTIVE EQUATIONS FOR ELASTOMERIC BEARINGS

The conventional methods for earthquake-resistant structural design use high strength or high ductility concepts to mitigate damage from seismic impacts. In the first case, corresponding to shear wall structures, generally the design is problematic in that their fundamental frequency of vibration is in the range of frequencies where earthquake energy is strongest. The second, the capacity design method, incorporates that a part of the energy transmitted into the structure by an earthquake is dissipated by plastic deformations. The capacity method mostly used for flexible structures like frames, provided that plastic deformations occur in structural elements, which are designed to undergo such large deformations. Therefore, the design of such yielding zones has to be planned carefully. An alternative approach consists in isolating the structure base from the ground by using rubber bearings. Some basic knowledge of seismic isolation principles using elastomeric bearings are presented in [Eibl et al.] and [Baur]. Also, an overview of the testing program for high damping rubber bearings (HDRB) under various loading conditions is given.

Beside the testing program, another task consisted of the formulation of a constitutive law which is able to describe the highly non-linear behavior of elastomeric bearings under cyclic loading numerically. For that purpose, an already existing finite visco-elastic material law of Simo-Taylor with an isotropic damage function was chosen. Due to the fact that elastomer is almost incompressible, the constitutive law is based on the uncoupling of the stress response into a linear volumetric and into a non-linear deviatoric part. The latter is described mathematically by a relaxation function and a distortion-supported damage function. To take into account the increase in stiffness at large strains, the original formulation of Simo-Taylor has been extended by adding a deviatoric strain-hardening function.

However, the verification of the model has clearly shown that the material behavior with the above-mentioned model can be numerically reproduced only in a very limited range. Therefore, an enhanced formulation became necessary. This formulation consists of the introduction of a strain- and time-dependent relaxation function and an extended strain-history function for describing the strain-hardening for the unloading case [Baur]. Thus, the enhanced fully three-dimensional constitutive law takes the form:

$$\sigma(t) = \underbrace{K^0 \ln J \mathbf{1}}_{\text{linear volumetric part}} + \underbrace{\int_0^t \mu(t-\tau) \frac{d}{d\tau} g(\varphi_D, \tau) h(\kappa, \tau) \text{dev}[\bar{\mathbf{C}}](\tau) d\tau}_{\text{non-linear deviatoric part}} \quad (3.1)$$

Here, the deformation gradient \mathbf{F} is decomposed into a pure volumetric $J^{1/3} \mathbf{1}$ and isochoric deformation $\bar{\mathbf{F}}$. Furthermore, the right Cauchy-Green-Tensor $\bar{\mathbf{C}}$ for the isochoric deformation is given by $\bar{\mathbf{C}} = J^{-2/3} \mathbf{C} = \bar{\mathbf{F}}^T \bar{\mathbf{F}}$. The relaxation function $\mu(t)$ and the time-dependent relaxation time $v(\phi, t)$ are defined as $\mu(t) = (G^0 + (G^0 - G^\infty) e^{-t/v})$ and $v(\phi, t) := \zeta_1 \cdot \phi^{\zeta_2}$ with $\phi(t) = \|\text{dev}[\bar{\mathbf{C}}](\tau)\|$ and $\phi(t) \in [0.05, 50.0]$. Here, G^0 and G^∞ are the short and the long time shear modulus. For describing the decrease of stiffness a damage function $g(\varphi_D, t) := (\beta + (1-\beta)(1 - e^{-\varphi_D/\alpha} / \varphi_D/\alpha))$ with an enhanced time history function $g \varphi_D(t) = \|\text{dev}[\bar{\mathbf{C}}](\tau)\|$ is implemented. Finally, a strain-hardening function $h(\kappa, t) := \delta \cdot \kappa + 1$ with $\kappa(t) = \|\text{dev}[\bar{\mathbf{C}}](\tau)\|^2$ and a scalar parameter δ is formulated to take into account the increase of the stiffness at large deformations. The material parameters that were used in the simulations are listed in table 3.1.

Table 3.1 Material parameters for the constitutive law of rubber

K^0 [MPa]	G^0 [MPa]	G^∞ [MPa]	ζ_1 [-]	ζ_2 [-]	α [-]	β [-]	δ [-]
2550	4.0	1.3	0.6	-0.9	0.1	0.3	0.02

The enhanced model is implemented in the FE-Code ABAQUS using an algorithm proposed by Kim et al.. In [Baur] it could be demonstrated, that the highly non-linear material behavior under various loading conditions can be realistically reproduced with the enhanced model.

4. SEISMIC PERFORMANCE OF A GIRDER BRIDGE

In dynamic simulations the influence of pier ductility and seismic isolation on the seismic bridge performance will be discussed on the example of a two span girder bridge (Figure 4). The study is confined on the seismic excitation in longitudinal direction. There are sliding bearings at both abutments, so that horizontal seismic forces are transferred at the two piers only. The total mass of the superstructure amounts 832 000 kg. Two models - one non-isolated and one base isolated model - were generated for the comparison. The first model considers the nonlinear behavior of the ductile piers with 48 fibre elements per pier. The second model considers the nonlinear behavior of two circular laminated elastomeric bearings at the piers. The bearing diameter is 800 mm and the elastomeric layers have a total thickness of 70 mm. The bearings are modeled with 200 continuum elements each. The remaining parts in both models are generated with beam elements and linear elastic material behavior.

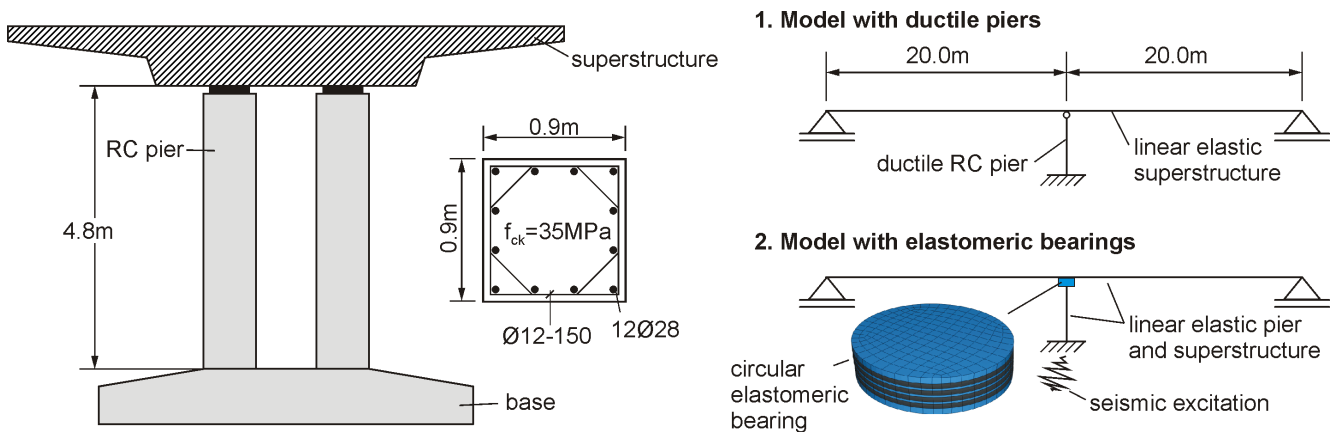


Figure 4 Girder bridge with RC pier cross section and the two FE-models

In order to consider the nonlinear behavior in the piers respectively in the elastomeric bearings realistic earthquake simulations have been performed using the nonlinear dynamic time history analysis in the FE-code ABAQUS. For that purpose spectrum compatible ground motion time histories have been generated using the SIMQKE code (Vanmarcke and Gasparini, 1976). Figure 5 (left) shows the normalized design spectrum according to the German code DIN 4149-1 for medium subsoil conditions. Three different ground motion histories were generated with SIMQKE that match closely the above mentioned design spectrum. The main difference between these ground motion representations is the random phase angle of their sinusoidal components. One representation is shown in Figure 5 (right) and for checking purposes its generated response spectrum (left). Each ground motion history was scaled by 1.0, 2.4, or 4.8 m/s² representing areas with low mean or high seismicity.

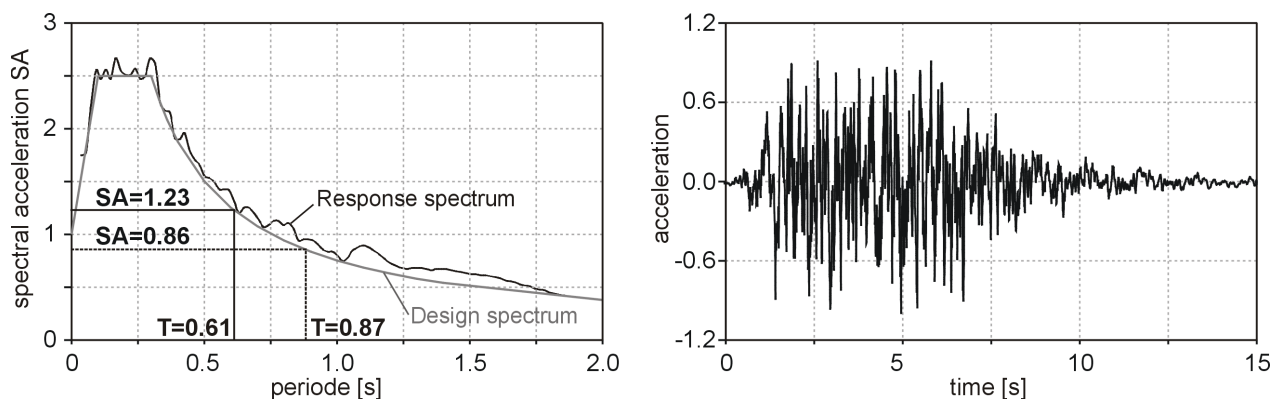


Figure 5 Normalized design spectrum (left), spectrum compatible accelerogram (right) and the corresponding response spectrum (left)

The fundamental eigenperiod of the non-isolated bridge was determined with a linear elastic model. Using a Young's modulus of $E_{cm} = 29\,900$ MPa for the piers results in a longitudinal eigenperiod of $T = 0.61$ s. According to Eurocode 8 cracked sections can be considered by a reduction of the concrete Young's modulus by 50%. The stiffness reduction results in an eigenperiod of $T = 0.87$ s. These periods lead to an ordinate of $SA = 1.23$ in the normalized design spectrum for the bridge with uncracked sections and $SA = 0.86$ for the bridge with cracked sections. According to Eurocode 8-2 the maximum base shear force can be approximated with the rigid deck model. Hence the maximum shear force per pier at the bridge with uncracked sections for low seismicity (1.0 m/s²) is:

$$F_{\max} = PGA \cdot SA \cdot \text{mass} = 1.0 \cdot 1.23 \cdot 416\,000/1000 = 512 \text{ kN} . \quad (2.1)$$

The shear force F_{\max} can analogously be calculated for mean and high seismicity and for the bridge with cracked sections. These results of the linear elastic analysis are shown in table 4.1, line 1 and 2.

For each PGA three nonlinear time history analysis were performed according to the three representations of ground motion from SIMQKE. For the ductile pier model the maximum base shear forces at one pier and the maximum relative displacements of the superstructure (pier deformations) were averaged for each PGA and written to table 4.1, line 3. An analogous approach was carried out for the seismic-isolated model. Here, the averaged maximum base shear force per pier and the averaged maximum horizontal deformation of the elastomeric bearing are written to table 4.1, line 4.

Table 4.1 Shear forces per pier and deformations from linear analysis and nonlinear simulations

Ground motion	Low (1.0 m/s ²)		Mean (2.4 m/s ²)		High (4.8 m/s ²)	
	d [mm]	F [kN]	d [mm]	F [kN]	d [mm]	F [kN]
Linear elastic (T=0.61s)	12	512	28	1 228	55	2 456
Linear elastic (T=0.87s)	17	361	39	866	78	1 731
Ductile pier model	19 ($\mu_{\Delta} \leq 1.0$)	394 ($q \approx 1.0$)	54 ($\mu_{\Delta} \approx 1.8$)	513 ($q = 1.7$)	118 ($\mu_{\Delta} \approx 3.9$)	587 ($q = 3.0$)
Seismic-isolated model	28	121	84	207	150	410

The forces in the piers with cracked sections from linear analysis are in comparison to uncracked sections ~30% smaller due to the reduced fundamental period while the displacements increase ~40%. Certainly forces and displacements increase linearly with the PGA of the input ground motion. In contrast to the linear analysis the forces in the ductile piers only increase slightly with increasing PGA. That is because at low seismicity almost no plastic deformations occur while at high seismicity large plastic deformations occur in concrete and steel. Therefore at low seismicity the maximum force at the ductile pier is in the range of the linear analysis with the better fit to the one with cracked sections. The behavior factor $q = F_{el}/F_u$ with the force F_{el} from the linear analysis with cracked sections and the force F_u from the ductile pier simulation is evaluated and shown in table 4.1, line 3. The behavior factor varies from $q = 1.0$ at low seismicity to $q = 3.0$ at high seismicity. That corresponds to an essentially elastic to ductile behavior according to Eurocode 8.

For low seismicity the displacements show a better agreement to the linear analysis with cracked sections, too. The amount of plastic deformations is quantified by the global displacement ductility $\mu_{\Delta} = d_u/d_y$ with the ultimate displacement d_u and the yield displacement d_y . Generally the displacement where the main bars start to yield and the global pier stiffness significantly reduces is defined as d_y . Preliminary static simulations have shown that the piers have an approximate elastic displacement of $d_y \approx 30$ mm. The evaluated displacement ductility is written to table 4.1, line 3. For bridges, which generally have relative high eigenperiods the behavior factor q equals the displacement ductility μ_{Δ} . The evaluation shows a good agreement between q and μ_{Δ} for low and mean seismicity. However for high seismicity μ_{Δ} is larger than q – the ductility demand increases faster. This is because the pier already shows concrete crushing with significant strain softening.

The nonlinear simulations with elastomeric bearings show smaller forces and larger displacements for all ground motions. The forces reduce by a factor 4 while displacements increase by a factor 1.5 to 2.0 compared to the linear analysis with cracked sections. The difference to the ductile pier simulations is most noticeable at low seismicity. While the piers at this bridge only reduce seismic forces via ductility starting from a specific level of seismic input the elastomeric bearings significantly reduce forces even at low seismicity. That is because the elastomeric bearings cause a seismic isolation that increase the bridge eigenperiod. However it must be kept in mind, that relative large displacements can occur due to non seismic forces, too.

Figure 6 (top) shows the hysteresis shear force per pier versus horizontal deformation of piers for the ductile-pier model for one representation of ground motion with different PGAs. In figure 6 (bottom) the corresponding hysteresis shear force per pier versus deformation of elastomeric bearing for the isolated model are shown. The ductile pier model for low excitation shows an extremely narrow hysteresis. The performance is almost linear elastic with no energy dissipation. With increasing PGAs the maximum force only becomes slightly larger while the area under the hysteresis significantly rises. That is the reason for the significant reduction of forces compared to the linear elastic analysis at mean to high seismic input. The hysteresis of the low-excitation simulation with the seismic-isolated model shows only moderate energy dissipation, too. However the average slope of the hysteresis respectively the global stiffness is smaller leading to the high reduction of forces. The hysteresis of the elastomeric bearing stays relatively narrow even for strong motions. Therefore the force reduction is almost independent from the PGA in contrast to the ductile pier model. The main effect of the elastomeric bearing is the reduction of global stiffness. It can beneficially be used for low ground motions while the effect of a ductile piers starts at a specified input - at the present girder bridge at mean seismicity. The performance of seismic isolated bridges can be further enhanced when the elastomeric bearing is combined with special damping devices.

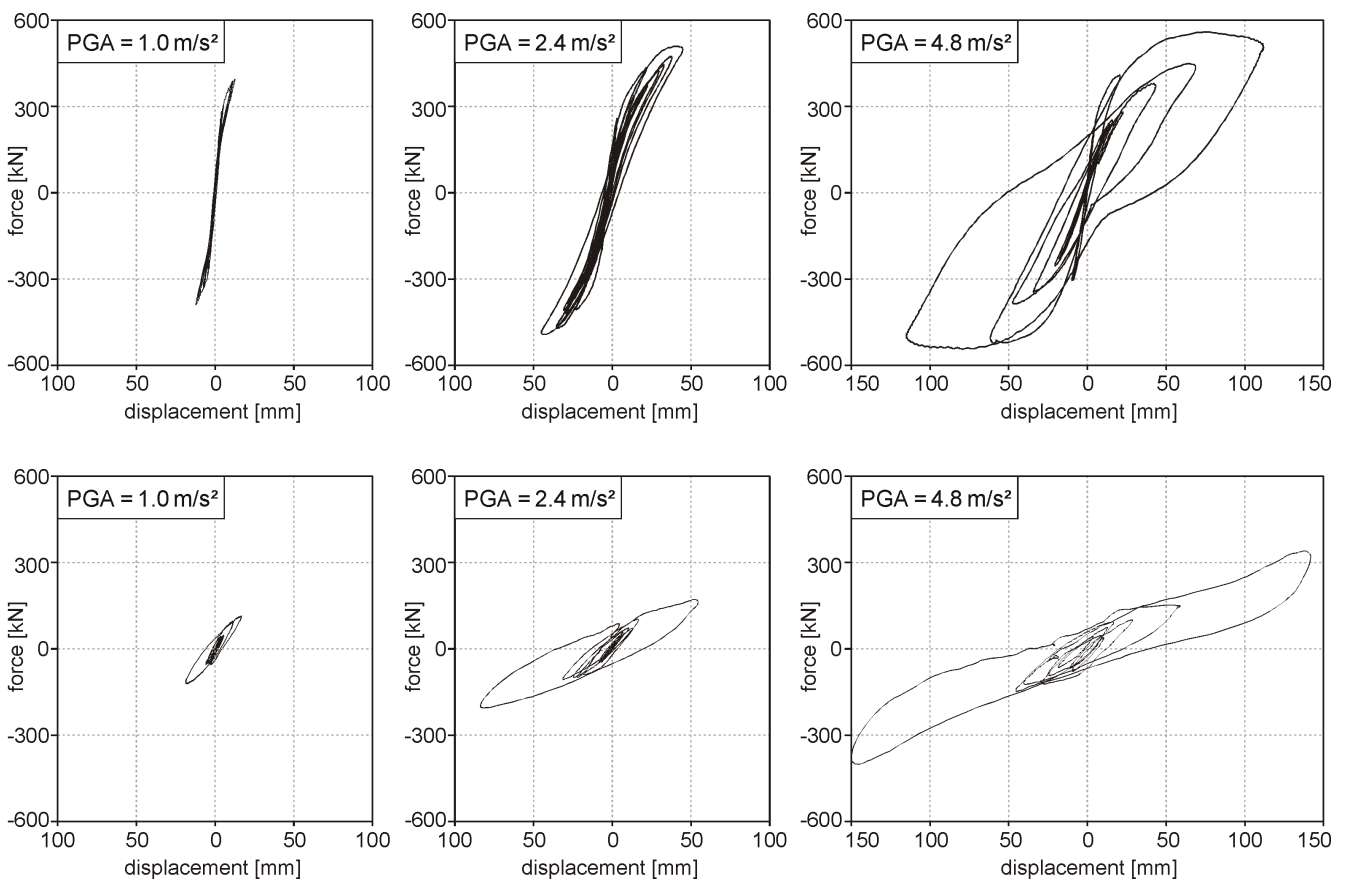


Figure 6 Hysteresis of ductile pier (top) and elastomeric bearing (bottom) for different PGAs

5. CONCLUSIONS

Two basic concepts of an earthquake-resistant structural design were investigated in the paper. First a ductile structural performance using plastic hinges in bridge piers and second an isolation of the structure by using rubber bearings. Numerical models were presented that can represent the above mentioned concepts in detail. The first model takes nonlinear material behavior of concrete and reinforcement into account. It considers bond-slip of the main bars and includes a nonlocal averaging of damage. The model shows good performance up to failure independently from mesh refinement. For the second model an already existing finite visco-elastic material law with an isotropic damage function was chosen. To take the stiffness increase at large strains into account, the formulation has been extended by a deviatoric strain-hardening function. With further extensions like a time-dependent relaxation function the highly nonlinear material behavior can realistically be reproduced under various loading conditions.

The difference of ductile pier performance versus seismic isolation with elastomeric bearings was investigated at a practical example. For this purpose dynamic simulations at a two span girder bridge have been carried out. The simulations have shown that a significant force reduction at bridges with ductile piers starts at a specific level of seismicity. At the considered girder bridge this reduction starts at mean seismicity. The main reason for the force reduction is the energy dissipation inside plastic hinges. At low seismicity where the ductile pier shows almost no energy dissipation the results agree best to simplified linear analysis when cracked sections are considered in linear analysis by reducing the Youngs-Modulus. The simulations at the seismic-isolated bridge have shown much smaller forces compared to the linear analysis even at low seismicity. The main effect of the elastomeric bearing is the reduction of global stiffness. Therefore the force reduction is significant at low seismicity but it only slightly increases with increasing seismicity. Elastomeric bearings can effectively be used for all levels of ground motion, but large displacements can occur even due to non seismic forces. The presented numerical models have shown an efficient runtime behavior so that it is possible to optimize the performance of new bridges or to investigate the performance of existing bridges.

REFERENCES

- Bazant, Z.P. and Planas, J. (1998) Fracture And Size Effect In Concrete And Other Quasibrittle Materials. CRC Press, Boston.
- Baur, M. (2003). Elastomerlager und nichtlineare Standorteffekte bei Erdbebeneinwirkung. Dissertation, University of Karlsruhe.
- Eibl, J., Hehn, K.H., Baur, M., Böhm, M., Schmidt-Hurtienne, B. (1996). Detailed numerical models of bearings. Brite- EuRam II. Project BE 7010, Technical Report No. 6, University of Karlsruhe.
- Eligehausen, R., Popov, E.P. and Bertero, V.V. (1983) Local Bond Stress-Slip Relationships of Deformed Bars under Generalized Excitations. Report UCB/EERC-83/23, University of California, Berkeley.
- Eurocode 8: Design Provisions for Earthquake Resistance of Structures, Part 2 bridges ENV 1998-1-2 (1994), ENV 1998-1-3 (1995), ENV 1998-2 (1994), CEN, European Committee for Standardization, Brussels.
- Fäcke, A. (2006). Numerische Simulation des Schädigungsverhaltens von Brückenfeilern aus Stahlbeton unter Erdbelastungen. Dissertation, University of Karlsruhe.
- Fäcke, A. and Baur, M. (2007) Assessment of Bridge Ductility for Earthquake Resistant Design. Munich Bridge Assessment Conference (MBAC).
- Kim, M., Gupta, A., Marchertas, A.H. (1991). Utilization of the Simo-Taylor constitutive model for the simulation of isolations bearings. SMiRT Conference, Transactions Vol. K, 169-174.
- Salse, E.A.B. and Fintel, M. (1973) Strength, Stiffness and Ductility Properties of Slender Shear Walls. 5th WCEE, Rom, 919-928.
- Simo, J. (1987). On a fully three-dimensional finite-strain viscoelastic damage model: Formulation and computational aspects. *Computer methods in applied mechanics and engineering* **60**, 153-173.